PRAMANA
— journal of
physics

Vol. 63, No. 1
July 2004
pp. 143–153

Spin dynamics of bilayer manganites

TAPAN CHATTERJI
Institut Laue-Langevin, BP 156, 38042 Grenoble Cedex 9, France
E-mail: chatt@ill.fr

Abstract. The results of inelastic and quasi-elastic neutron scattering investigations on the 40% hole-doped quasi-2D bilayer manganites $La_{1.2}Sr_{1.8}Mn_2O_7$ have been reviewed. The complete set of exchange interactions have been determined on the basis of a localized Heisenberg model. However, the spin wave dispersion in $La_{1.2}Sr_{1.8}Mn_2O_7$ shows softening close to the zone boundary and are also heavily damped especially close to the zone boundary and deviate from that expected for a simple Heisenberg model. A minimal double exchange model including quantum corrections can reproduce these effects qualitatively but falls short of quantitative agreement.

Keywords. Spin waves; neutron scattering; colossal magnetoresistance.

PACS Nos 75.30.Ds; 75.25.+z; 72.15.Gd

1. Introduction

The discovery of colossal magnetoresistance (CMR) in the quasi-two-dimensional (quasi-2D) bilayer manganite $La_{2-2x}Sr_{1+2x}Mn_2O_7$ [1] generated a lot of investigations to understand the microscopic mechanism of this phenomenon. Together with the high temperature superconducting cuprates with layered structures they formed a class of materials in which hole doping drives the parent antiferromagnetic insulator to either a superconductor with high critical temperature T_C or a metallic ferromagnet showing CMR. The reduced dimension is another common ground in the present class of materials with perovskite-like structures. Due to the reduced dimensionality of this bilayer manganite, its electronic and magnetic properties are expected to be different from those for the well-studied infinite-layer manganite [2]. The reduced dimensionality in fact enhances the CMR effect, albeit at the cost of decreasing the ferromagnetic transition temperature.

2. Spin-waves in bilayer manganites

2.1 *Spin-wave dispersion at low temperatures*

The bilayer manganite $La_{1-2x}Sr_{1+2x}Mn_2O_7$ shows a large CMR effect close to T_C and the CMR is anisotropic as is expected for a layered structure. Figure 1 shows

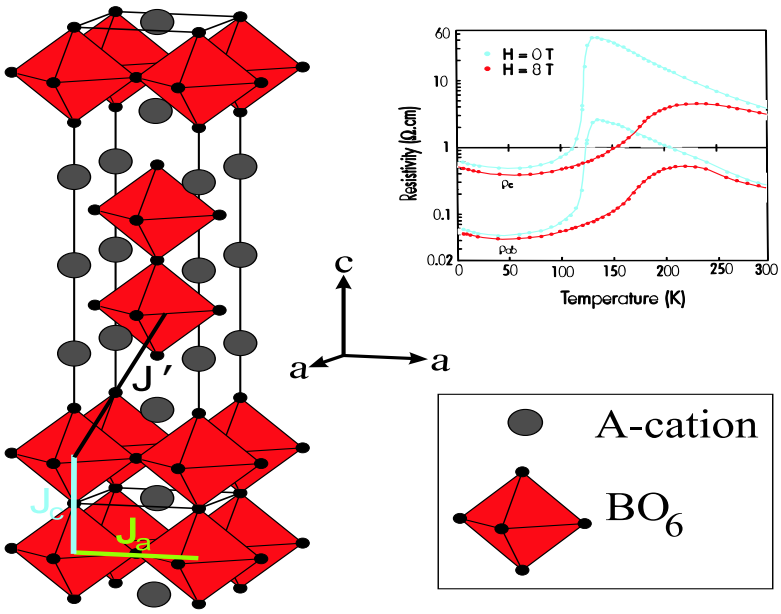

Figure 1. Crystal structure of $La_{1.2}Sr_{1.8}Mn_2O_7$ and the important exchange interactions. The temperature dependence of the resistivity of the $La_{1.2}Sr_{1.8}Mn_2O_7$ single crystal measured in the a–b plane and parallel to the c-axis of the orthorhombic I4/mmm crystal structure at applied magnetic field $H = 0$ and 7 tesla.

the temperature dependence of resistivity of the $La_{1.2}Sr_{1.8}Mn_2O_7$ single crystal measured in the a–b plane and parallel to the c-axis of the orthorhombic I4/mmm crystal structure at applied magnetic field $H = 0$ and 7 tesla. The resistivity has been measured on a part of the large single crystal of dimensions $5 \times 5 \times 25$ mm^3.

Figure 1 also shows the crystal structure of the bilayer manganite and the three important exchange interactions: (1) the intra-layer exchange interaction J_a between the nearest-neighbor Mn atoms along the a-axis, (2) the intra-bilayer exchange interaction J_c between the nearest-neighbor Mn atoms along the c-axis belonging to the two layers of the bilayer and (3) the inter-bilayer exchange interaction J' between the nearest-neighbor Mn atoms belonging to different bilayers. The spin waves in bilayer manganite $La_{1.2}Sr_{1.8}Mn_2O_7$ have been investigated by us by inelastic neutron scattering [3–5] on the triple-axis spectrometers of the Institute Laue-Langevin, Grenoble. The spin waves in bilayer manganites have also been investigated by several other authors [6–10]. One expects $La_{1.2}Sr_{1.8}Mn_2O_7$ to behave like a quasi-2D magnetic system. The spin waves involving intra-bilayer exchange interactions J_a and J_c are expected to have much higher energy than those involving inter-bilayer exchange interaction J'. So we used thermal triple-axis spectrometers to investigate the former spin waves and cold triple-axis spectrometers to investigate the latter. Also one expects two spin-wave branches, acoustic and

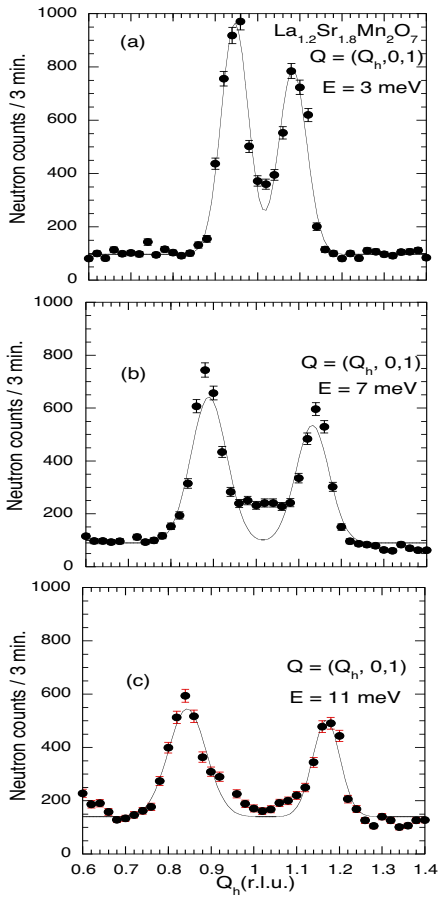

Figure 2. Q scans along [1 0 0] at $T = 1.6$ K for different constant energy transfers through the reciprocal point $Q = (1, 0, 1)$ which is a zone center.

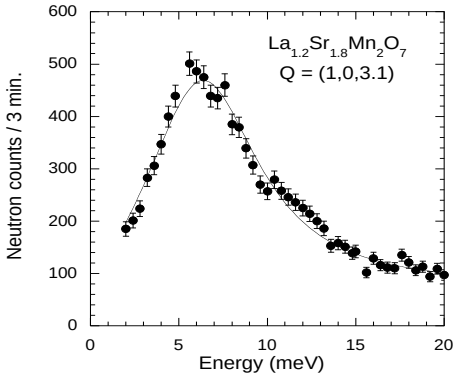

Figure 3. Energy scan at $Q = (1, 0, 3.1)$ at $T = 1.6$ K which shows a peak at $E \approx 6$ meV.

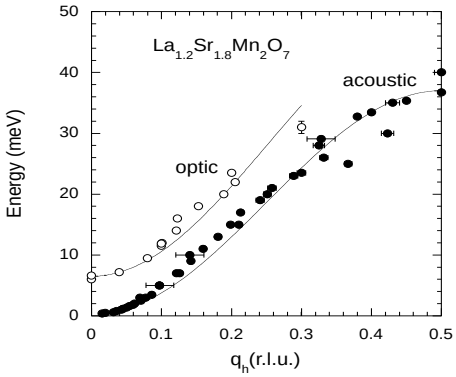

Figure 4. Spin-wave dispersion of the acoustic and the optic branches of $La_{1.2}$ $Sr_{1.8}$ Mn_2O_7 along [1 0 0].

optic, due to the presence of two Mn atoms in the primitive unit cell related by the inversion center leading to magnetic bilayers. The spin-wave dispersion was measured by both energy and Q scans. Figure 2 shows Q scans along [1 0 0] at $T = 1.6$ K for different constant energy transfers through the reciprocal point $Q = (1, 0, 1)$ which is a zone center. The two peaks observed on both sides of the zone center are acoustic spin waves. The dispersion of the acoustic spin waves along [1 0 0] is clearly seen. Figure 3 shows energy scan at $Q = (1, 0, 3.1)$ at $T = 1.6$ K which shows a peak at $E \approx 6$ meV.

This peak has been identified as the optic spin-wave branch. The dispersion of the optic spin-wave branch along [1 0 0] has also been measured. Figure 4 shows the dispersions of both the branches along [1 0 0]. The continuous curves are fit

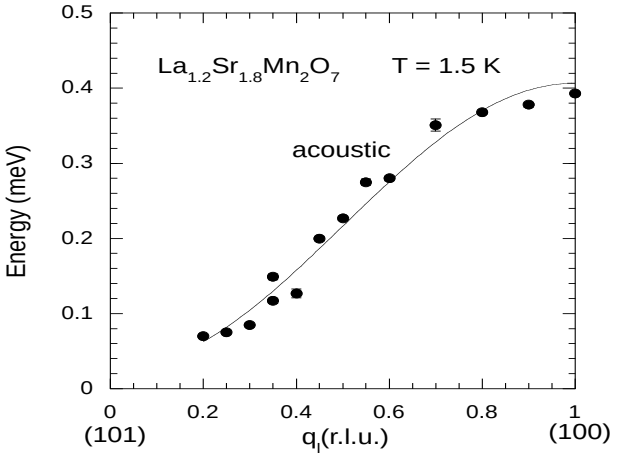

Figure 5. Spin-wave dispersion of the acoustic branches of $La_{1.2}Sr_{1.8}Mn_2O_7$ along [0 0 1].

to the localized Heisenberg model. This fit gives the nearest-neighbor intra-layer interaction $SJ_a = 8.6 \pm 0.2$ meV along [1 0 0]. The spin-wave gap has been determined from the low-q dispersion by fitting $E = \Delta + Dq^2$ giving an energy gap of $\Delta = 0.266 \pm 0.001$ meV and the spin-wave stiffness constant $D = 167.9 \pm 0.1$ meV Å^2. The optic spin-wave energy gap directly gives the intra-bilayer exchange interaction $SJ_c = 3.1 \pm 0.2$ meV along the c-axis. The ratio of the in-plane exchange interaction to the intra-bilayer exchange interaction $J_a/J_c = 2.8$. This large ratio came as a surprise initially. However, it has been realized that the population of the $d_{z^2-3r^2}$ and $d_{x^2-y^2}$ orbitals play a crucial role in determining these exchange interactions. Also this exchange ratio depends strongly on the doping level. The fit of the experimental dispersions along [1 0 0] to the localized Heisenberg model is not very good. It is known that the localized Heisenberg model is not appropriate for the spin waves in manganites. They are better described by the double exchange model. The double exchange model can be mapped to a localized Heisenberg model in the classical limit only for a very large Hund's coupling. Figure 5 shows the dispersion of the acoustic spin-wave branch along [0 0 1] measured by a cold triple-axis spectrometer. The spin-wave band width along [0 0 1] is only about 0.4 meV, which is much smaller than that along [1 0 0] (37 meV). The continuous curve is the fit to the localized Heisenberg model which gives the inter-bilayer exchange interaction $SJ' = 0.057 \pm 0.002$ and a spin-wave gap $\Delta = 0.04 \pm 0.02$ meV.

The q_l-dependence spin-wave cross-section of the acoustic and optic branch can be well-described by

$$\left(\frac{\mathrm{d}^2\sigma}{\mathrm{d}\Omega \mathrm{d}E}\right)_{m,\pm 1} = \frac{k_\mathrm{f}}{k_\mathrm{i}}(\gamma r_0)^2 \frac{(2\pi)^3}{2N_m v_0}\frac{g^2 S}{4}(1+\hat{\mathbf{Q}}_z^2) f^2(\mathbf{Q}) \times \mathrm{e}^{-2W(\mathbf{Q})} \sum_m \sum_{\boldsymbol{\tau}_\mathbf{q}} \left\langle n_q + \frac{1}{2} \mp \frac{1}{2} \right\rangle \delta(\mathbf{Q} \mp \mathbf{q} - \boldsymbol{\tau}) \times \delta[E \mp \hbar\omega(\mathbf{q})][1 \pm \cos(2zcQ_l)], \quad (1)$$

where $\gamma r_0 = 0.539 \times 10^{-12}$ cm, $\mathbf{Q} = \mathbf{k}_\mathrm{i} - \mathbf{k}_\mathrm{f}$ is the momentum transfer, $\mathbf{k}_\mathrm{i}$ and $\mathbf{k}_\mathrm{f}$ are the wave vectors of the incoming and scattered neutrons, $f(Q)$ is the magnetic form factor of the Mn ion, $\mathrm{e}^{-2W(\mathbf{Q})}$ is the Debye–Waller factor, n_q is the Bose factor, $\boldsymbol{\tau}$ is the reciprocal vector, m denotes a mode, z is the z-coordinate of the Mn ion, c is the lattice parameter along the z direction, i.e., perpendicular to the bilayers. The sign in the last factor refers to the acoustic (+) and optic (−) spin wave modes, whereas the other signs denote the creation and annihilation of a spin wave, respectively. The crystal structure investigation of $La_{1.2}Sr_{1.8}Mn_2O_7$ gave $z = 0.0964 \pm 0.0001$ and the lattice parameters are $a = 3.864 \pm 0.002$, $c = 20.160 \pm 0.006$ Å. We note that $2zc = 3.88$ is close to $a \approx c/5$. The spin-wave intensity will oscillate as a function of Q_l peaking at $l = 0$, 0.58, etc. and becoming zero at $Q_l = 2.59$, 10.36, etc. for the acoustic mode. The phase of the optic mode is shifted by π, so the intensity of this branch is zero at $l = 0$, 0.58, etc. and becomes maximum at $Q_l = 2.59$, 10.36, etc. Figure 6 shows the Q_l variation of the spin-wave cross-section after correcting for the form factor, along $\mathbf{Q} = (1, 0, Q_l)$ for a constant energy transfer of 6 meV (acoustic mode) and also that $\mathbf{Q} = (1.13, 0, Q_l)$ for a constant energy transfer of 7 meV (optic mode). The continuous curve is a fit of the intensity with eq. (1). There is only a scale factor in the fit and the agreement is excellent.

We already commented that the dispersion of the spin waves of the compound $La_{1.2}Sr_{1.8}Mn_2O_7$ cannot be fitted well by the localized Heisenberg model in the entire q range. The deviation of the spin-wave dispersion from the localized Heisenberg model can be seen in figure 7. The continuous curve shows the calculated dispersion where the gap Δ and the exchange interaction J_a have been kept fixed to the values obtained by fitting only the low-q data. It is seen that the calculated dispersion has a zone-boundary energy of about 46 meV, whereas the experimental value of the zone-boundary energy is only about 37 meV. There is a softening of the spin waves close to the zone boundary. The softening of the spin waves close to the zone boundary seems to be a generic feature of all doped ferromagnetic manganites. The minimal double exchange model developed by us [11] does not describe the zone boundary softening adequately. In order to describe the zone boundary softening in ferromagnetic manganites one needs to invoke the orbital and/or lattice degrees of freedom.

Another important deviation of the spin excitations in the compound $La_{1.2}Sr_{1.8}Mn_2O_7$ from the localized Heisenberg model is the strong damping of the spin waves especially closer to the zone boundary. This is already illustrated in figure 3. The continuous curve in figure 3 is a fit of the intensity by a damped harmonic oscillator function. The damping Γ obtained from the fit is, $\Gamma = 4.0 \pm 0.2$ meV, which is much larger than the instrumental resolution that is about 1–1.5 meV. This shows that the optic mode is already damped at the zone center. The damping increases as the momentum transfer q is increased. We show in figure 8 energy scans at $T = 1.5$ K close to the zone boundary corresponding to $Q = (1.40, 0, 5)$, $(1.45, 0, 5)$, and $(1.50, 0, 5)$. The full-width at half-maximum of these energy scans are as high as about 25 meV compared to the instrumental resolution that is about 5 meV. We have investigated spin-wave damping of $La_{1.2}Sr_{1.8}Mn_2O_7$ as a function of momentum transfer. Figure 9 illustrates the spin-wave damping of $La_{1.2}Sr_{1.8}Mn_2O_7$. The figure has been constructed from the energy scans at $T = 1.5$ K at about ten q values equally spaced in the range $0 \leq q \leq 0.5$, i.e., in the range from zone center

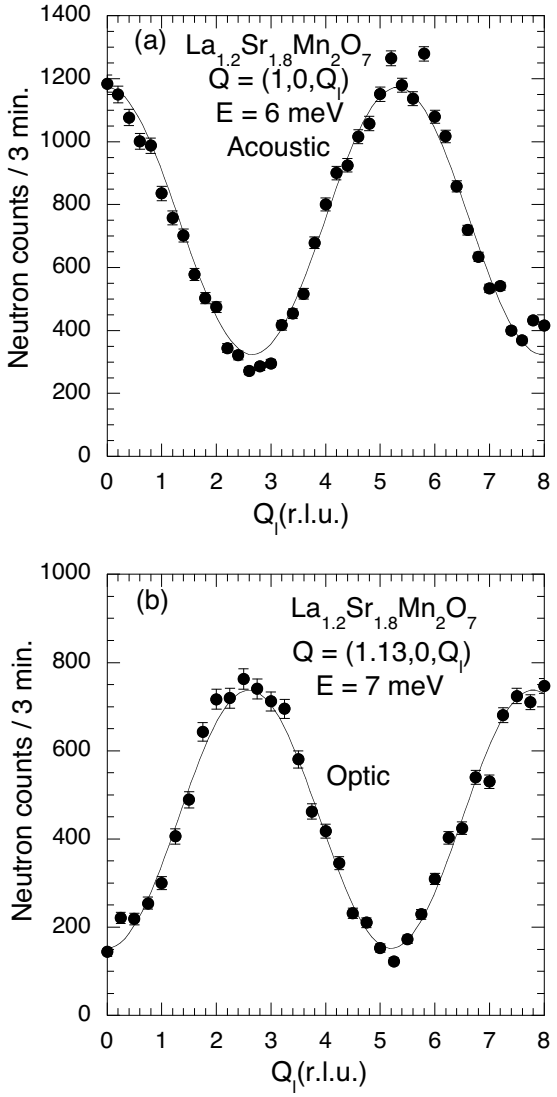

Figure 6. Q_l variation of the spin-wave cross-section after correcting for the form factor, along (**a**) $\mathbf{Q} = (1, 0, Q_l)$ for a constant energy transfer of 6 meV (acoustic mode) and also that (**b**) along $\mathbf{Q} = (1.13, 0, Q_l)$ for a constant energy transfer of 7 meV (optic mode).

to the zone boundary. The damping of the spin waves especially close to the zone boundary is another generic feature of the hole-doped ferromagnetic manganites. The minimal DE model [11] gives damping that is much less than that observed experimentally. To describe the spin-wave damping one may also has to invoke orbital and/or lattice degrees of freedom. The A-site disorder has also been considered as a possible source of damping [12].

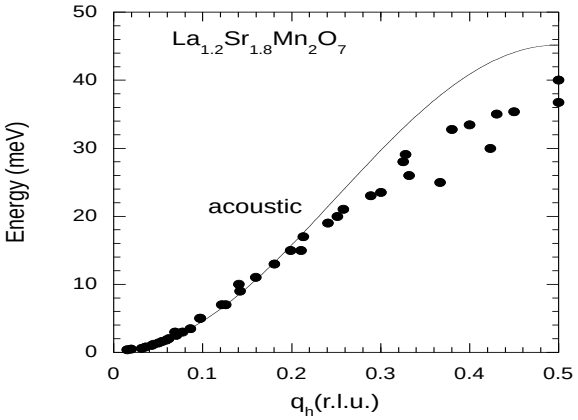

Figure 7. Dispersion of the acoustic branch along [1 0 0]. The continuous curve shows the dispersion calculated from eq. (1) in which the gap Δ and the exchange interaction J_a have been kept fixed to the values obtained by fitting only the low-q data.

2.2 *Nature of the ferromagnetic ground state in hole-doped manganites*

The nature of the ferromagnetic ground state in hole-doped manganites is still debated. There are several unusual features of the ferromagnetic metallic state in hole-doped manganites. The undoped parent compound is an antiferromagnetic insulator. It is known that for the undoped parent compound, strong electron correlations, Hund's rule coupling and the Jahn–Teller effect are very important. The hole-doped manganites with a doping level x has a fraction x of the Mn ions in the Mn^{4+} state and the fraction $(1-x)$ in the Mn^{3+} state. Due to the hoping of the e_g electron from the Mn^{3+} site to the neighboring Mn^{4+} site, the mixed valent manganite can be metallic. The hopping is proportional to the probability amplitude that the initial and final states have the maximum spin $S = 2$ (Hund's rule coupling). Therefore gain in the kinetic energy of the e_g electron is largest for parallel or ferromagnetic configuration of the neighboring spins. The ground state is expected to be a ferromagnetic metal because of the kinetic energy gained by the e_g electron moving parallel to the aligned t_{2g} spins. At higher temperature they become progressively disordered. Therefore, the e_g electrons can no longer propagate well and there is a transition to a paramagnetic insulating phase. The itinerant e_g electron carries along with it the Jahn–Teller distortion (polaron) which aids the transition or may be even its cause. The colossal magnetoresistance which is observed near the transition is due to the fact that a magnetic field, by partially aligning the spins makes it easier for the electrons to move. The above explanation of the ferromagnetic metallic ground state and the colossal magnetoresistance exhibited by them at the ferromagnetic phase transition is however only qualitative. There are several aspects of the hole-doped manganites which are not well-understood: (1) The metallic state has resistivities which correspond to an electron mean free path smaller than a lattice spacing. (2) The magnitude of the colossal magnetoresistance is much larger than expected. A magnetic field of a few tesla, which is

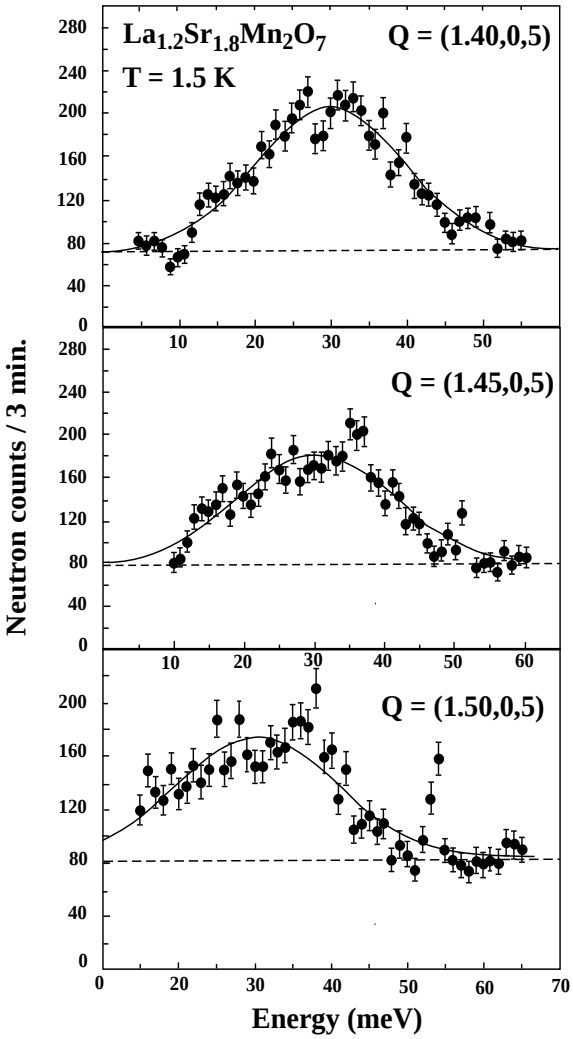

Figure 8. Energy scans at $T = 1.5$ K close to the zone boundary corresponding to $Q = (1.40, 0, 5)$, $(1.45, 0, 5)$, and $(1.50, 0, 5)$.

of the order of a few degrees K, makes a large difference in electronic transport at temperatures of a few hundred degrees K. (3) The paramagnetic-to-ferromagnetic phase transition usually takes place below the insulator-to-metal transition temperature at which the electrical resistivity shows a maximum. The metal–insulator transition in the hole-doped manganites is the most important property which distinguishes them from the classical ferromagnetic metals. (4) The zone-boundary softening (deviation from the dispersion expected in the Heisenberg model) observed in the spin-wave dispersion has not yet been accounted for successfully. (5) The huge damping of the spin wave close to the zone boundary is also not explained quantitatively.

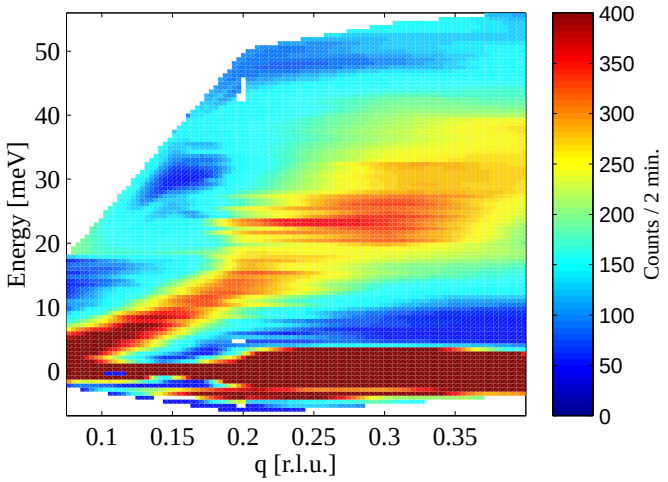

Figure 9. E–q plot of spin-wave dispersion of $La_{1.2}Sr_{1.8}Mn_2O_7$ along [1 0 0]. The spin waves are particularly damped at higher values of q close to the zone boundary.

2.3 *Comparison with infinite-layer manganites and other itinerant magnetic systems*

The hole-doped metallic ferromagnetic manganites are expected to have itinerant character. Itinerant metallic ferromagnets such as iron and nickel have been the subjects of investigation for more than half a century [13]. The spin waves in itinerant ferromagnets have been investigated by inelastic neutron scattering. The neutron scattering investigation of the spin dynamics of the doped ferromagnetic manganites has made considerable progress. We have attempted to summarize the data obtained by neutron scattering in hole-doped manganites along with those of classical metallic itinerant ferromagnets. Mook [13] has suggested the ratios D/kT_C and E_{ZB}/kT_C as criteria for the itinerancy of the magnetic electrons. Here E_{ZB} is the energy of the zone boundary magnon. These two ratios have high values for itinerant electron systems like Fe and Ni and are small for localized systems like EuO and EuS. Table 1 gives the ordering temperature T_C, spin-wave stiffness D, zone-boundary magnon energy E_{ZB} and criteria for itinerancy D/kT_C and E_{ZB}/kT_C of the infinite-layer and bilayer manganites along with those of other known itinerant and localized magnetic materials. Comparing the ratios D/kT_C and E_{ZB}/kT_C of different materials from Table 1 we see that the doped ferromagnetic manganites which are close to the composition at which CMR effects are maximum, are of rather itinerant character. Especially the bilayer manganite is more itinerant than the infinite-layer manganites. In fact the ratio D/kT_C for $La_{1.2}Sr_{1.8}Mn_2O_7$ is as high as 15.3 compared to 10.1 of Ni. The ratio E_{ZB}/kT_C for $La_{1.2}Sr_{1.8}Mn_2O_7$ is 3.35 which is lower than that for Ni (6.43) but higher than that of Pd_2MnSn (1.83) and Pt_3Mn (2.05).

Table 1. Ordering temperatures T_C, spin-wave stiffness D, zone-boundary magnon energy E_{ZB} and criteria for itinerancy D/kT_C and E_{ZB}/kT_C of the infinite layer and bilayer manganites along with those of other known itinerant and localized magnetic materials [5,13].

Sample	T_C (K)	D (meV Å^2)	E_{ZB} (meV)	D/kT_C (Å^2)	E_{ZB}/kT_C
$La_{0.95}Ca_{0.05}MnO_3$	123.0(3)	4.5(1)	1.6[0 0 1]	0.42	0.15
$La_{0.92}Ca_{0.08}MnO_3$	26.0(3)	7.3(1)	1.6[0 0 1]	0.67	0.15
$La_{0.67}Ca_{0.33}MnO_3$	250	170		7.9	
$La_{0.85}Sr_{0.15}MnO_3$	235	95(2)	56[0 1 0]	4.6	2.76
$La_{0.7}Sr_{0.3}MnO_3$	355				
$La_{0.7}Ba_{0.3}MnO_3$	350	152(3)	32[1 0 0]	5.04	1.06
$La_{0.7}Pb_{0.3}MnO_3$	355	133.7	35[1 0 0]	4.37	1.14
$La_{1.2}Sr_{1.8}Mn_2O_7$	128	169	37[1 0 0]	15.3	3.35[1 0 0]
Ni	631	550	350	10.1	6.43
Fe	1021	281	800	3.19	9.1
MnSi	40	52		15.8	
Ni_3Al	41	85		24.0	
Fe_3Pt	504	80		1.84	
Pd_2MnSn	190	100	30	6.10	1.83
Pt_3Mn	453	215	80	5.51	2.05
EuO	69	12	6	2.01	1.02
EuS	10.6	2.6	2.3	1.82	1.61

3. Concluding remarks

We have shown that the spin-wave dispersion in the ferromagnetic bilayer manganite $La_{1.2}Sr_{1.8}Mn_2O_7$ is not at all given by nearest-neighbor Heisenberg localized model. The spin waves show softening close to the zone boundary and are also heavily damped. The minimal DE model [11] for the spin waves shows very similar softening and damping effects qualitatively but falls short of explaining the experimental results quantitatively. One may have to include the orbital and lattice degrees of freedom for a quantitative explanation of the observed softening and damping in $La_{1.2}Sr_{1.8}Mn_2O_7$.

Acknowledgement

The author wishes to thank P Thalmeier, L P Regnault, Nic Shannon, A Hiess, P Vorderwisch, R Suryanarayanan, G Dhalenne and A Revcolevschi for collaboration.

References

[1] Y Moritomo, A Asamitsu, H Kuwahara and Y Tokura, *Nature* **380**, 141 (1996)
[2] Y Tokura (Eds.), *Colossal magnetoresistive oxides* (Gordon and Breach, Amsterdam, 2000)

[3] T Chatterji, P Thalmeier, G J McIntyre, R van de Kamp, R Suryanarayanan, G Dahlenne and A Revcolevschi, *Europhys. Lett.* **46**, 801 (1999)
[4] T Chatterji, L P Regnault, P Thalmeier, R Suryanarayanan, G Dahlenne and A Revcolevschi, *Phys. Rev.* **B60**, R6965 (1999)
[5] T Chatterji, L P Regnault, P Thalmeier, R van de Kamp, W Schmidt, A Hiess, P Vorderwisch, R Suryanarayanan, G Dahlenne and A Revcolevschi, *J. Alloys Compounds* **326**, 15 (2001)
[6] H Fujioka, M Kubota, K Hirota, H Yoshizawa, Y Moritomo and Y Endo, *J. Phys. Chem. Solids* **60**, 1165 (1999)
[7] K Hirota, S Ishihara, H Fujioka, M Kubota, H Yoshizawa, Y Moritomo, Y Endoh and S Maekawa, *Phys. Rev.* **B65**, 64414 (2002)
[8] G Chaboussant, T G Perring, G Aeppli and Y Tokura, *Physica* **B276–278**, 801 (2000)
[9] T G Perring, D T Androja, G Chaboussant, G Aeppli, T Kimura and Y Tokura, *Phys. Rev. Lett.* **87**, 217201 (2001)
[10] S Rosenkranz, R Osborn, L Vasiliu-Doloc, J F Mitchell, J W Lynn and S K Sinha, *J. Appl. Phys.* **87**, 5816 (2000)
[11] Nic Shannon, T Chatterji, F Ouchini and P Thalmeier, *Euro. Phys. J.* **B27**, 287 (2002)
[12] Y Motome and N Furukawa, *J. Phys. Soc. Jpn.* **71**, 1419 (2002)
[13] H Mook, *Spin waves and magnetic excitations I* edited by A S Borovik-Romanov and S K Sinha (Elsevier, Amsterdam, 1988) p. 425